ARTICLE
Journal of Cellular Biochemistry 114:56–66 (2013)

Journal of Cellular Biochemistry

Novel Frameshift Mutation in the p16/INK4A Tumor Suppressor Gene in Canine Breast Cancer Alters Expression From the p16/INK4A/p14ARF Locus

Farruk M. Lutful Kabir, Payal Agarwal, Patricia DeInnocentes, Jishan Zaman, Allison Church Bird, and R. Curtis Bird*

Department of Pathobiology, AURIC—Auburn University Research Initiative in Cancer, College of Veterinary Medicine Auburn University, Auburn, Alabama 36849

ABSTRACT

The INK4 family of cyclin-dependent kinase inhibitors (CKI) encode important cell cycle regulators that tightly control cell cycle during G1 to S phase. These related genes are considered tumor suppressors as loss of function contributes to the malignant phenotype. Expression of CKIs p16, p14ARF, or p15 were defective in six different canine mammary tumor (CMT) cell lines compared to normal thoracic canine fibroblasts. This suggests CKI defects are frequently responsible for neoplastic transformation in canine mammary carcinomas. p16 and p14ARF are two alternatively spliced products derived from the canine p16/INK4A/p14ARF gene locus. Despite omissions in the published p16 transcript and canine genome and the presence of GC-rich repeats, we determined the complete coding sequence of canine p16 revealing a deletion and frameshift mutation in p16 exon 1α in CMT28 cells. In addition, we determined canine p14ARF mRNA and protein sequences. Mapping of these mutations uncovered important aspects of p16 and p14ARF expression and defects in CMT28 cells shifting the p16 reading frame into p14ARF making a fusion protein that was predicted to be truncated, unstable and devoid of structural and functional integrity. This data describes an important neoplastic mechanism in the p16/INK4A/p14ARF locus in a spontaneous canine model of breast cancer. J. Cell. Biochem. 114: 56–66, 2013.

KEY WORDS: p16/INK4A; p14ARF; CANINE MAMMARY CANCER; MUTATION; ANIMAL MODEL

Tumor suppressor genes play vital roles in controlling cell cycle, replication, recombination, signal transduction, differentiation, and aging [Oesterreich and Fuqua, 1999]. Tumor suppressors directly control cell proliferation by regulating cell cycle check-points promoting neoplasia when they acquire mutations [Tripathy and Benz, 1992; Kinzler and Vogelstein, 1997]. Cell cycle progression is regulated by cyclin/cyclin-dependent kinases (CDKs) whose activities are regulated by CKIs [Pines and Hunter, 1991; Morgan, 1997]. All CKIs are tumor suppressors. The INK4 CKI family consists of p16/INK4A, p15/INK4B, p18/INK4C, and p19/INK4D [Vidal and Koff, 2000]. INK4 proteins inhibit assembly of CDK4/6 with cyclin D preventing Rb phosphorylation promoting inactivation of E2F transcription factors required for S phase [Weinberg, 1995]. Genes of the INK4 family are evolutionarily and functionally related and are thought to have evolved from a common ancestor through gene duplication [Sharpless, 2005; Agarwal et al., 2012]. The p16/INK4A/p14ARF locus (human chromosome 9p21, canine chromosome 11) encodes two different transcripts (p16 and p14ARF) that are alternatively spliced and translated into different proteins with distinct cell cycle regulatory and tumor suppressor functions [Ruas and Peters, 1998; Fosmire et al., 2007; Agarwal et al., 2012]. p16 and p14ARF share a large overlapping sequence encoded by exons 2 and 3 but different alternatively spliced first exons (exon 1α and 1β, respectively) resulting in 2 different reading frames (Fig. 1A).

Both p16 and p14ARF are tumor suppressor genes but have quite different functions [Kim and Sharpless, 2006]. p16 inhibits G1/S phase transition by inhibiting CDK4/6–cyclinD1 complexes [Russo

Financial support: Animal Health and Disease Research Fund.
Conflict of interest: The authors state that there are no conflicts of interest.
Farruk M. LutfulKabir and Payal Agarwal contributed equally to the manuscript.
*Correspondence to: Dr. R. Curtis Bird, PhD, Department of Pathobiology, Auburn University, 164 Greene Hall, College of Veterinary Medicine, Auburn, AL 36849-5519. E-mail: birdric@auburn.edu
Manuscript Received: 10 July 2012; Manuscript Accepted: 17 July 2012
Accepted manuscript online in Wiley Online Library (wileyonlinelibrary.com): 25 July 2012
DOI 10.1002/jcb.24300 • © 2012 Wiley Periodicals, Inc.

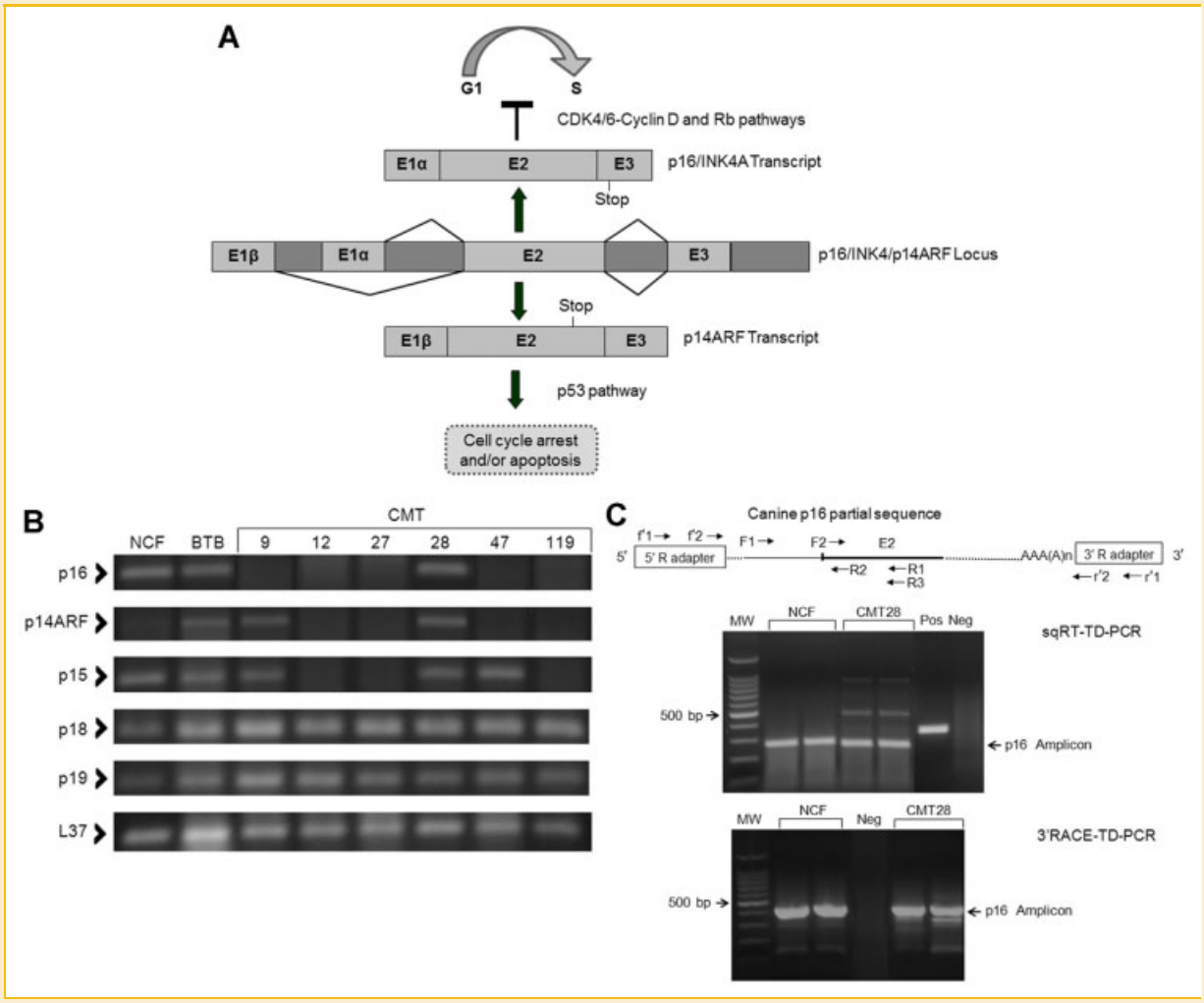

Fig. 1. CMT expression of INK4 CKIs. A: Alternative splicing from the p16/INK4A/p14ARF locus. The p16/INK4A/p14ARF locus encodes p16 and p14ARF transcripts that share common exons, E2 and E3, but different alternatively spliced first exons: E1α and E1β (splice junctions thin lines). p16 and p14ARF transcripts are translated into proteins with different functions regulating cell cycle (T-bars and arrows indicate spliced products and cell cycle effects). B: INK4 CKI expression in CMT cells. RNA extracted from each cell line was used as templates in sqRT-PCR to amplify INK4-encoded mRNAs. Expression of 5 INK4 genes (p16, p14ARF, p15, p18, p19) in 8 canine cell lines (CMT9, 12, 27, 28, 47, 119, and NCF, BTB) were evaluated. L37 served as control transcript. C: Amplification of p16 from NCF and CMT28 by TD-PCR. Top: schematic representing experimental design indicating p16 PCR primers. Primer pair F1 (forward) and R1 (reverse) were designed for amplification of 5′ upstream region by sqRT-TD-PCR. 3′-RACE PCRs were designed for amplification of downstream region of the gene using primer pairs F1, r′1 and F2, r′2. 5′-RACE reactions employed different primer pairs f′1, R3 and f′2, R2. Continuous line indicates partial canine p16 sequence including partial exon 2 (E2 thick line). Dotted line represents sequence absent from published p16 sequences. Arrows indicate position/orientation of primers on the canine p16 sequence. Middle: expression of p16 upstream region (right arrows) in two passages of NCF and CMT28 cells evaluated by sqRT-TD-PCR. Bottom: amplification of 3′-region of p16 in the same cells by 3′-RACE-TD-PCR. MW: 100 bp molecular weight markers, left arrow: 500 bp fragment. Positive (Pos) and negative (Neg) control PCR reactions.

et al., 1998] while p14ARF stabilizes p53 protein disrupting interactions with the E3 ubiquitin ligase mdm2 [Boehme and Blattner, 2009]. Under conditions requiring p53 activation, p14ARF binds and blocks mdm2 releasing and stabilizing p53 [Boehme and Blattner, 2009]. Functional effects of p14ARF are not limited to p53 as p14ARF has been implicated in vascular regression in developing eye [McKeller et al., 2002] and arrest of cell cycle in embryo fibroblasts in the absence of p53 [Weber et al., 2000]. p14ARF also binds E2F-1, MDMX, HIF1-α, topoisomerase I, c-myc, and nucleophosmine [Boehme and Blattner, 2009]. Previous studies have demonstrated p16 can suppress proliferation when transfected into human and canine tumor cell lines [Jin et al., 1995; Spillare et al., 1996; Campbell et al., 2000; DeInnocentes et al., 2009]. Defects in INK4 genes have been associated with cancers in humans and dogs including melanoma, osteosarcoma, and mammary carcinoma [Levine and Fleischli, 2000; Koenig et al., 2002] and p16/INK4A defects are second in frequency only to p53 for human malignancies [Baylin et al., 1998].

Mammary cancers are the most common tumors in unspayed female dogs, comprising approximately 52% of all neoplasms a majority of which are diagnosed as malignant [Ahern et al., 1996; Withrow and MacEwen, 1996; Rutteman et al., 2001]. Canine

mammary carcinomas provide a high level of similarity in genetics, pathology, and environmental exposure when compared to human breast cancer [DeInnocentes et al., 2006; Migone et al., 2006]. Like humans, expression of canine cell proliferation, and cell cycle regulatory genes are frequently altered in breast cancer [Ahern et al., 1996; DeInnocentes et al., 2006]. Because humans and dogs share the same environment, and many disease characteristics, dogs provide excellent intermediate models of breast cancer in women [Smith and Bird, 2010].

We previously demonstrated defective expression of p16 mRNA in three canine mammary tumor cell lines (CMT12, CMT27, and CMT28) [DeInnocentes et al., 2009]. Although CMT28 cells expressed p16 mRNA they did not express detectable protein (Agarwal et al., unpublished data) however, the cause of this defect is unknown and complicated due to missing coding sequence from the published canine genome (CanFam 2.0 genome assembly, http://www.ensembl.org) and GC-rich repeats within the coding region causing difficulty in primer design and amplification [Lindblad-Toh et al., 2005]. We report the development of technologies for mapping p16 and p14ARF genetic defects and analysis of mRNA and protein sequences important for evaluation of p16 in the development of canine breast cancer. We also evaluate the expression profiles and defects for all INK4 gene family members in a panel of independently derived spontaneous canine breast cancer cell lines. This is the first report of the complete canine p16/INK4A and p14ARF mRNA expression and mRNA and protein sequences including those missing from the canine genome.

METHODS AND MATERIALS

CELL CULTURE AND LYMPHOCYTE ISOLATION

CMT cell lines were derived from female dogs of different breeds (CMT9, CMT12 from Poodle, CMT 27 from German Shepherd, CMT28 from mixed breed, CMT47 from Miniature Schnauzer, and CMT119 from Golden Retriever) with spontaneous mammary carcinomas or adenocarcinomas. Normal thoracic canine fibroblasts (NCF) were developed as previously described and a mammary epithelium-derived cell line (BTB) was developed from normal canine mammary epithelium. Cell lines were grown as previously described [Wolfe et al., 1986; DeInnocentes et al., 2006]. Peripheral blood mononuclear cell (PBMC) populations were isolated from Grey Wolf blood as previously described [Bird et al., 2008, 2011].

RNA EXTRACTION

Total RNA was isolated from cells (<80% confluence) by phenol–chloroform extraction according to the manufacturer's instructions (RNA STAT-60; Tel-Test, Inc.). RNA pellets were air-dried and stored (−80°C). Pellets were resuspended in diethylpyrocarbonate-treated water for PCR assays. Concentration and purity of RNA was determined by absorbance at 260 nm [You and Bird, 1995].

PRIMER DESIGN

Primers were designed for INK4 genes using Vector NTI primer design software (Invitrogen, Table I). Published canine INK4 sequences were aligned with sequences from other mammalian species and primers designed from highly conserved unique regions.

TABLE I. Primer Sequences Designed for INK4 Genes

Gene	Primers (forward/reverse)	Primer sequences (5′–3′)
p16	F1 (3′-RACE gene specific outer/ forward primer)	CAGCATGGAGCCTTCGGCTGACTG
	F2 (3′-RACE gene specific inner/ forward primer)	CAGCACCACCAGCGTGTCCAGGAAG
	R1 (Reverse)	CAGGTCATGATGATGGGCAGC
p14ARF	R2 (5′-RACE gene specific inner/ reverse primer)	TCGGCACAGTTGGGCTC
	R3 (5′-RACE gene specific outer/ reverse primer)	CCACCAGCGTGTCCAGGAAG
	Forward	CGAGTGAGGGCTTTCGTGGTG
	Reverse	ACCACCAGCGTGTCCAGGAAG
p15	Forward	GTGCGGCAGCTCCTGGAAG
	Reverse	CCAGCGTGTCCAGGAAGCC
P18	Forward	CGCTGCAGGTTATGAAACTT
	Reverse	GCAGGTTCCCTTCATTATCC
P19	Forward	GCTGCAGGTCATGATGTTTG
	Reverse	GAGCATTGACATCAGCACCA
L37	Forward	AAGGGGACGTCATCGTTCGG
	Reverse	AGGTGCCTCATTCGACCGGT

SEMI-QUANTITATIVE REVERSE TRANSCRIPTION-PCR (sqRT-PCR) AND TOUCHDOWN-PCR (TD-PCR)

Gene expression was analyzed by sqRT-PCR using mRNA templates in semi-quantitative assays at limiting template dilution and minimum amplification number [DeInnocentes et al., 2009]. sqRT-PCR was performed in one reverse transcription (RT) step (Icycler, Bio-Rad) and then amplification using specific primers. PCR protocol consisted of RT (48°C, 45 min), denaturation (94°C, 2 min), and amplification cycles (p18 and p19 25 cycles, p15 30 cycles, 35 cycles for TD-PCR) composed of denaturation (94°C, 1 min), annealing for 30 s (67°C for p14ARF and p15; 60°C for p18 and p19) and elongation (68°C, 1 min). Amplification was followed by extension (68°C, 7 min).

The TD-PCR protocol was RT (48°C, 45 min), denaturation (94°C, 2 min), and 10 cycles of denaturation (94°C, 1 min), annealing 1 min (primer annealing temperature plus 10°C decreasing 1°C/cycle) and elongation (68°C, 1 min) followed by 25 cycles PCR amplification as described (annealing 65°C for p16, 60°C for p14ARF). TD-annealing temperature range for p16 was 75–65 and 70–60°C for p14ARF [Korbie and Mattick, 2008]. PCR products were analyzed semi-quantitatively on 2.5% agarose electrophoresis gels comparing L37 control gene and 100 bp DNA markers.

RAPID AMPLIFICATION OF cDNA ENDS (RACE)

RNA was extracted from NCF and CMT28 cells and 3′-RACE-PCR performed (RLM-RACE kit, Ambion) according to the manufacturer's instructions. First stand cDNA was synthesized from RNA by RT (48°C 1 h) using the 3′-RACE adapter ligated to the 3′-poly(A)tails. cDNA was amplified using gene-specific primers (F1 and F2) and 3′-RACE primers (r′1 and r′2) complementary to anchored 3′-RACE adapters (Fig. 1C top). Outer 3′-RACE-PCR was first performed using F1 and r′1 primers. Inner nested 3′-RACE-PCR was performed using nested primers F2 and r′2 and outer 3′-RACE product as template. In 5′-RACE, adapters were ligated to 5′-RNA

ends prior to RT. 5′-RACE-PCRs were performed using gene-specific reverse primers (R2 and R3) and 5′-RACE primers (f′1 and f′2) complementary to anchored 5′-RACE adapters.

RACE-PCRs were optimized using thermostable GC-rich template-adapted polymerase (AccuPrime GC-rich DNA polymerase, Invitrogen) in TD-PCR. RACE-TD-PCR cycle profiles were denaturation (95°C, 3 min), TD (10 cycles of denaturation 95°C, 30 s, annealing at temperature plus 10°C and decreasing 1°C/cycle, 30 s, elongation at 72°C, 30 s) followed by 25 amplification cycles (denaturation, 95°C, 30 s, annealing at temperature from previous TD step, 30 s, elongation, 72°C, 30 s) and extension at 72°C, 7 min. Inner 3′/5′-RACE-PCR products were analyzed by 2.0% agarose gel electrophoresis.

TA-CLONING, SEQUENCING, ALIGNMENT AND PROTEIN STRUCTURAL ANALYSIS

Amplicons (identified by apparent molecular weight) were gel purified and cloned into TA-cloning vector pCR2.1 according to manufacturer's instruction (Invitrogen). Successfully propagated clones were identified by restriction endonuclease digestion and 1.5% agarose gel electrophoresis. Cloned amplicons were isolated, processed and sequenced (MGH DNA Sequencing, Cambridge, MA). Amplicon sequences were subjected to BLAST analysis (http://blast.ncbi.nlm.nih.gov/) to confirm authenticity. Canine p16 and p14ARF sequences were aligned with published p16 and p14ARF sequences using Vector NTI AlignX (Invitrogen). Dendrograms were generated from multiple alignments applying a neighbor-joining algorithm (ClustalW, Vector NTI).

Protein sequences were predicted from coding sequences and aligned and instability indices calculated (ExPASyProtParam algorithm) [Gasteiger et al., 2005]. Protein motifs and native folding were predicted and compared using motif/structure prediction and fold recognition databases (Phyre V0.2 protein fold recognition server, 3D-PSSM Fold Recognition Server, Swiss-Model InterproScan) [Kelley et al., 2000; Zdobnov and Apweiler, 2001; Kelley and Sternberg, 2009].

RESULTS

DIFFERENTIAL EXPRESSION OF INK4 TUMOR SUPPRESSORS IN CMT MODELS

INK4 mRNA expression was analyzed for a panel of six different CMT cell lines derived from canine primary carcinoma and adenocarcinomas [Wolfe et al., 1986; DeInnocentes et al., 2006]. Because p16, p14ARF and p15 encode repetitive GC-rich sequences, design and optimization of unique primers and protocols was challenging (Table I) but sqRT-PCRs (following optimization by TD-PCR) were performed to uniquely detect INK4 transcripts [DeInnocentes et al., 2006]. Following optimization, expression profiles for INK4 genes were determined for CMT cells (Fig. 1B). Expression of 1 or more of p16, p14ARF, and p15 mRNAs were absent in most CMT cell lines. p16 mRNA expression was defective in all CMT cell lines except CMT28 cells compared to p14ARF and p15, which were expressed in 2 or 3 of the CMT cell lines, respectively. p16 and p14ARF share common exons 2 and 3 requiring that PCR reactions include primers specific for each gene designed from the unique first exons. Primers had to avoid repeated and common sequences and also employed noncoding strand primers from shared exon 2. The success of this strategy was demonstrated by the ability to discriminate each transcript in different CMT cell lines where only 1 of p16 and p14ARF was expressed or where only p15 was expressed among these cell lines. CMT9 expressed p14ARF and p15 but not p16 while CMT47 expressed p15 but not p16 or p14ARF and NCF expressed p16 but not p14ARF (Fig. 1B). These results demonstrate that each primer pair amplified only the transcript intended and could distinguish expression of each gene. This was confirmed by sequencing multiple reactions (data not shown). Where p16 and p15 were expressed, levels detected in CMT cells were comparable to levels observed in normal primary NCFs.

Expression of p18 and p19 were both upregulated in all of the CMT cell lines evaluated when compared to NCFs (Fig. 1B). This supports a previous report that human tumor-derived cell lines, also frequently mutated for p16 and p15, expressed few detectable defects in p18 and p19 [Zariwala and Xiong, 1996]. A canine mammary epithelium-derived cell line (BTB) expressed all of the INK4 genes at comparable levels to those observed in CMT cells and at levels frequently higher than those in NCFs. NCFs expressed all of the INK4 genes except p14ARF, which was not expressed and p19, which was only just detectable. Levels for the expressed genes in NCFs were conspicuously lower compared to CMT cells with the exception of p16 and p15.

Similar differential expression patterns for the INK4 genes, including expression defects in p16, were also observed in primary canine cells directly isolated from several breast carcinoma biopsy samples (data not shown) implying that these genetic defects are not likely an artifact of culture in vitro. These results suggested that p16, among all members of the INK4 gene family, was the most frequently defective in almost all of the CMT cell lines followed by p14ARF and then p15. CMT9 and CMT47 cells provided examples where malignant cells were defective for p16 alone or combined with p14ARF.

AMPLIFICATION OF p16 FROM NCF AND CMT28 CELLS

The coding sequence of canine p16 is incomplete in the published canine genome (AF234176) so RACE-strategies to discover missing exon 1α sequences were employed (Fig. 1C upper). Since p16 and p14ARF share the exon 2/3 region, primers were designed from conserved unique upstream p16 sequences avoiding p14ARF homology. Optimized touchdown (TD) sqRT-PCR generated p16 amplicons of ~270 bp from NCF and CMT28 cells (Fig. 1C middle) that were isolated and cloned. To amplify p16 transcript 3′ ends, 3′-RACE-TD-PCR was performed using gene-specific forward primers (F1 and F2) and 3′-RACE reverse primers (r′1 and r′2, Fig. 1C). Outer 3′-RACE-TD-PCR was performed using gene-specific outer primer F1 and 3′-RACE outer primer r′1 from cDNA templates. Inner (nested) 3′-RACE-TD-PCR was then carried out (primers F2 and r′2). 3′-RACE primers (r′1 and r′2) were complementary to adapter sequences ligated to mRNA poly(A)tails (Fig. 1C upper). Nested 3′-RACE-PCR generated an amplicon of ~400 bp (Fig. 1C bottom) covering most of the downstream region of p16 mRNA including the 3′-terminal poly(A)tail (see below).

SEQUENCING AND ALIGNMENTS REVEAL NOVEL LESION IN CMT28 p16 EXON 1α

Cloned amplicons and 3′-RACE-PCR products were sequenced and authenticity of p16 sequences confirmed by BLAST analysis (http://blast.ncbi.nlm.nih.gov/Blast.cgi). Complete p16 sequences from NCF and CMT28 cells were generated from separate upstream and downstream sequences that aligned with published p16 sequences derived from other mammals and partial canine p16 sequences (Fig. 2A). Alignment allowed identification of conserved ATG start codons, three exon regions and 3′poly(A)tails of canine p16 from both cell lines. Most striking, p16 from CMT28 but not from NCF, was found to encode a 17 bp deletion in exon 1α, providing direct evidence for a genetic defect in p16 in canine mammary cancer that would result in a predicted frameshift mutation.

Evolutionary relationships between p16 coding sequences from NCF, CMT28 cells, and other vertebrates were determined (Fig. 2B). Dendrograms comparing p16 sequences revealed evolutionary relationships among mammalian species rooted on more distant chicken p16. Rodent and pig sequences were clustered separately from human and canine sequences. Canine p16 sequences (NCF, CMT28) were more closely related to human p16 than other mammals suggesting high levels of conservation among these species. Predicted p16 protein sequences were also aligned and were highly conserved. Unlike p16 mRNAs, the CMT28 $p16_{mut}$ protein sequence was poorly aligned with other p16 protein sequences after the first 7 amino acids resulting in premature termination with a truncated sequence compared to other p16 proteins including NCF (Figs. 2A and 3).

p14ARF mRNA SEQUENCE AND PREDICTION OF CANINE p14ARF ORF

Similar strategies for identification of canine p14ARF sequences were employed designing new upstream primers unique to p14ARF exon 1β (Fig. 1A). p14ARF amplicons (267 bp) were synthesized from CMT28, NCF, and primary lymphocytes from Grey Wolf (*Canis lupus*). All amplicons were cloned and sequenced from each source. Amplified NCF, CMT28, and Grey Wolf p14ARF nucleotide sequences were aligned with the p14ARF ORF from *Canis lupus familiaris* and other mammals (Fig. 4A). The conserved ORFs (exon 1β/exon 2 boundary) were predicted and differences from human peptide sequences determined. The CMT28 sequence was identical to the published canine p14ARF gene sequence with 1 nucleotide difference between NCF and CMT28 p14ARF resulting in 1 amino acid change (Fig. 4A, open box). This non-conservative glutamine (polar) to arginine (basic) substitution likely represents an allelic difference in normal dogs. The glutamine variant is more likely the ancestral form as it was present in Grey Wolf. Comparing canine p14ARF protein sequences to human p14ARF revealed 84.2% nucleotide similarity resulting in 31 amino acid differences (76.2% similar). Surprisingly, in all canid exon1β sequences, there was a deletion of 9 nucleotide base pairs compared to human and Opossum 3 nucleotides of which were also deleted in mouse and pig p14ARF sequences. This makes canid p14ARF 3 amino acids shorter than human/Opossum p14ARF and 1 amino acid shorter than mouse/pig. Dendrograms comparing canid p14ARF mRNA and protein sequences with those from human and other mammals did not show clustering of dog with human and rodent sequences likely due to the deletion/insertions in exon 1β (Fig. 4B).

MUTATION IN CMT28 p16 CHANGES THE READING FRAME TO p14ARF EXON 2 RESULTING IN AN UNSTABLE TRUNCATED PROTEIN

CMT28 $p16_{mut}$ was predicted to translate an altered reading frame due to a 17 bp deletion in exon 1α (Fig. 5A). The first 22 base pairs of p16 exon 1α were conserved followed by the remainder of exon 1α, which was read out of frame generating unique sequence. Following the exon 2 boundary, reading frame was shifted to that of p14ARF exon 2 (Fig. 5A). This suggests CMT28 $p16_{mut}$ is predicted to translate into a hybrid-protein composed of p16 (mutated exon 1α) and p14ARF (exon 2) resulting in an aberrant and likely dysfunctional protein (Fig. 5B,C). Translation of CMT28 $p16_{mut}$ would result in shorter peptide sequences (104 amino acids) compared to wild type NCF p16 (151 amino acids, Fig. 3). The CMT28 $p16_{mut}$ protein sequence was found to be unstable compared to wild type protein (high calculated instability index, ProtParam algorithm) [Gasteiger et al., 2005] suggesting that if CMT28 cells produced a truncated/altered p16/p14ARF fusion protein it would most likely be rapidly degraded. This supports previous experimental evidence that CMT28 cells do not express detectable p16 protein by Western blot (Agarwal et al., unpublished data). Since the majority of the CMT28 $p16_{mut}$ peptide sequence would be identical to p14ARF exon 2 and the remainder of exon 1α was unique, except the first 7 amino acids, it is unlikely that p16 antibodies would recognize the CMT28 $p16_{mut}$ peptide (Fig. 5B). A schematic of CMT28 $p16_{mut}$ protein indicates how different it is from wild type p16 and p14ARF consisting of an initial short amino acid sequence from p16 exon 1α (E1′α), a large conserved region from p14ARF exon 2 (due to the frameshift mutation) and a middle unique sequence ($E1'\alpha_{mut}$) unique to the putative fusion peptide (Fig. 5C).

FRAMESHIFT MUTATION IN CMT28 p16 EXON 1α DISRUPTS PREDICTED STRUCTURAL AND FUNCTIONAL INTEGRITY

Because frameshift mutation was predicted to cause deletion and truncation of CMT28 $p16_{mut}$ protein, both wildtype and mutant p16

Fig. 2. Alignment of canine and other mammalian p16 sequences. A: Canine p16 amplicon sequences from NCF (#JQ796919) and CMT28 (#JQ796920) were aligned and compared to published p16 sequences (human #L27211, chimpanzee #NM_001146290, mouse #AF044336, pig #AJ316067), p16 exon 2 sequences (human #U12819, pig #AJ242787, cat #AB010807) and predicted partial p16 sequences from the canine genome (#AF234176). Alignments revealed a highly conserved ATG start codon, identical (dark shaded), and conserved (light shaded background) regions. Exon 2 (E2) and exon 3 (E3) boundaries are indicated (bent arrows). A 17 bp deletion was identified in CMT28 exon 1α (E1α) from p16 alignments (large arrow). p16 sequences from both cell lines terminated in 3′ end poly(A)tails but included different stop codons (boxed TGA codons). Asterisks indicate canine p16 mRNAs sequenced in this study. B: p16 sequence dendrograms. A neighbor-joining algorithm was used to calculate a rooted relationship dendrogram for p16 coding sequences. The dendrogram compares published p16 sequences from human, chimpanzee, pig, Norway rat (#NM_031550), and mouse rooted on domestic chicken (#NM_204434) with p16 from canine NCF and CMT28 cells. Values in parentheses show the length of each branch proportional to number of nucleotide differences.

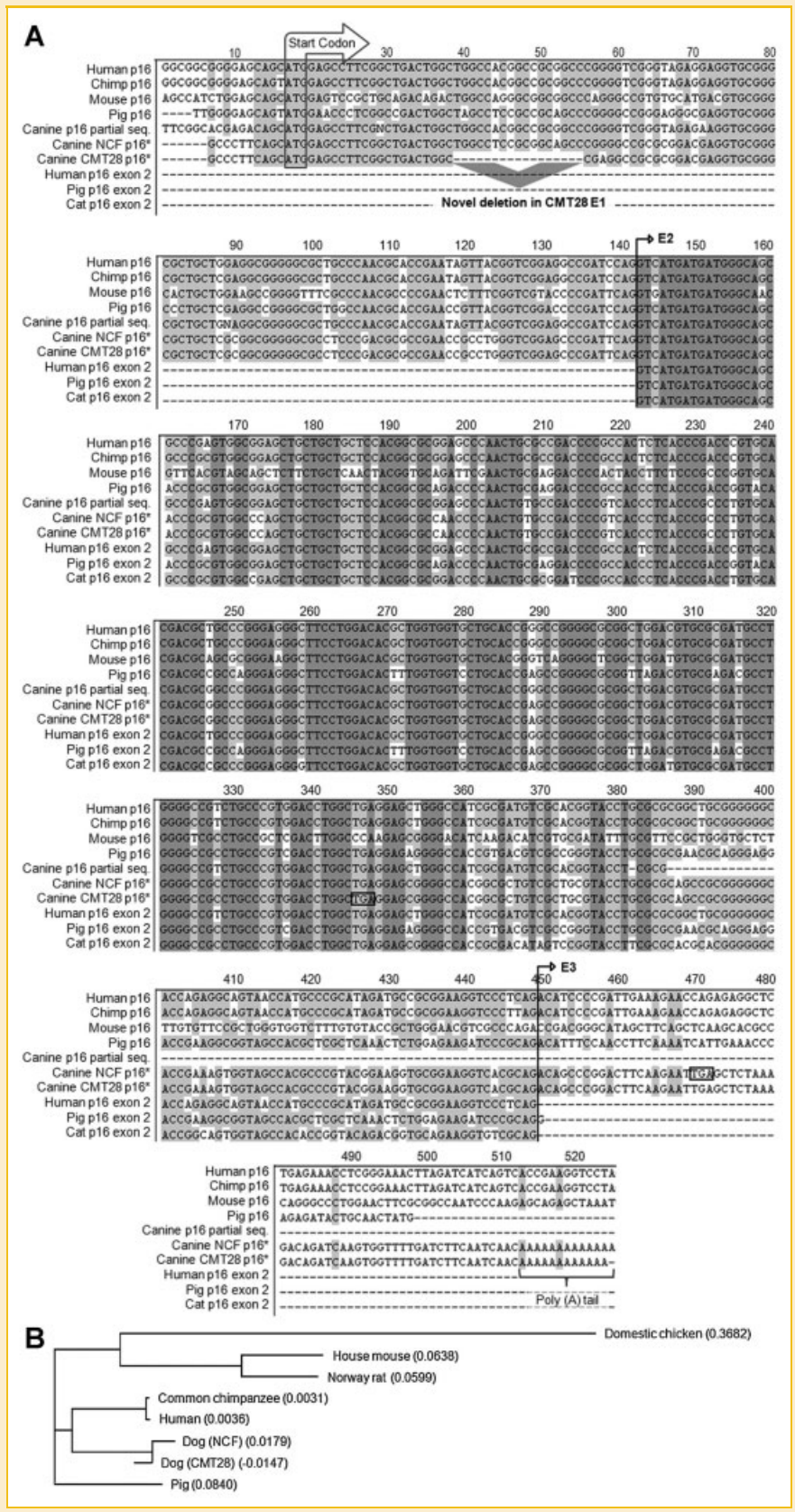
A
Start Codon
Human p16
Chimp p16
Mouse p16
Pig p16
Canine p16 partial seq.
Canine NCF p16*
Canine CMT28 p16*
Human p16 exon 2
Pig p16 exon 2
Cat p16 exon 2
Novel deletion in CMT28 E1
E2
E3
Poly (A) tail
B
Domestic chicken (0.3682)
House mouse (0.0638)
Norway rat (0.0599)
Common chimpanzee (0.0031)
Human (0.0036)
Dog (NCF) (0.0179)
Dog (CMT28) (-0.0147)
Pig (0.0840)

Fig. 2.

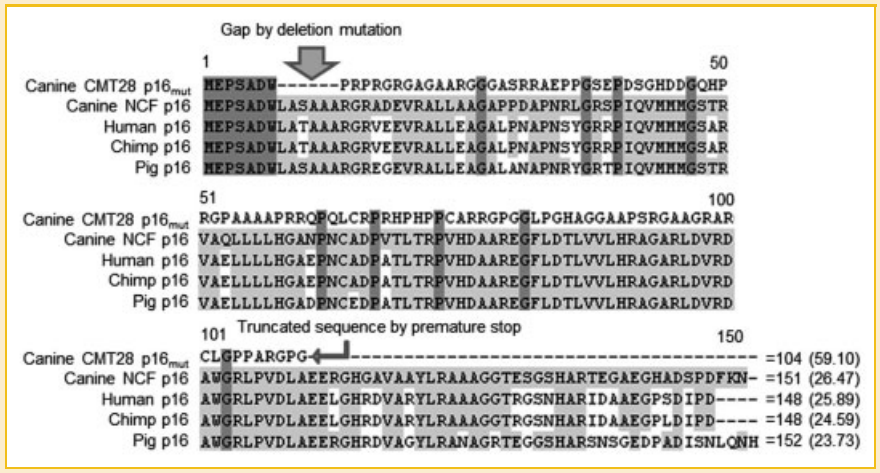

Fig. 3. Comparison of predicted CMT28 $p16_{mut}$ protein sequence with wild type sequences from NCF and other mammals. p16 sequences from NCF, CMT28 cells, and other p16 sequences were translated and aligned. Instability index of each p16 protein sequence (ExPASyProtParam algorithm) is indicated (parentheses) after the length of each protein sequence (amino acid number). Instability indices less than 40 were predicted to be relatively stable whereas indices greater than 40 indicated relatively unstable proteins. Shading of sequence alignments as noted (Fig. 2).

protein sequences were analyzed using the protein motif/structure prediction tool (Phyre V0.2) [Kelley and Sternberg, 2009] to predict functional protein folding motifs (Fig. 6). Sequences were further analyzed characterizing wildtype canine p16 protein as encoding a family of beta-hairpin–alpha-hairpin ankyrin repeats and predicting a model of folded structure (3D-PSSM, InterProScan and ScanProsite tools) [Kelley et al., 2000; Zdobnov and Apweiler, 2001] (Fig. 6A,B). No recognizable hairpin or repeat structures were identified in the CMT28 $p16_{mut}$ protein. Moreover, wildtype NCF p16, but not CMT28 $p16_{mut}$ protein models, revealed potential ligand binding sites (3DLigandSite server data not shown) [Wass et al., 2010]. Because CMT28 $p16_{mut}$ protein shares a large overlapping amino acid sequence with canine p14ARF, we also investigated whether it could undergo p14ARF-like structural folding or form similar functional motifs using the same protein motif and fold recognition bioinformatics tools. Wildtype p14ARF sequences predicted a folded structure and a unique N-terminal motif not shared with $p16_{mut}$ protein (Fig. 6A,B). The CMT28 $p16_{mut}$ sequence revealed neither the folded structure with ankyrin repeats comparable to p16 nor p14ARF-like N-terminal folding (Fig. 6A,B).

DISCUSSION

Canine cancers are excellent intermediate models for study of human cancers because many have remarkably similar etiologies to human cancers and dogs share the same environments with their owners. Spontaneous canine cancers bridge biological distances between induced mouse tumors and human cancers [Bird et al., 2008]. CMT cells have been characterized for tumor suppressor gene expression defects including p16, p21, and p53 and for defects in oncogenes such as c-*erb*B-2 and c-*yes* [DeInnocentes et al., 2006; Bird et al., 2008; DeInnocentes et al., 2009]. It is important to characterize these defects to determine how closely they reflect defects found in human breast cancer. Continued research on CMT models builds validation and reinforces the strength of the model particularly for development of novel therapeutic strategies.

All canine mammary tumor cell lines used in this study are highly transformed lines derived from different dog breeds with clinical cases of spontaneous mammary carcinoma [Wolfe et al., 1986; DeInnocentes et al., 2006]. Evaluation of INK4 expression profiles in the canine mammary tumor model suggested defects in these genes were extremely common. We have shown that while p16, p14ARF, and p15 expression were defective/absent in most CMT cell lines, p18 and p19 were overexpressed in these tumor cell lines compared to NCF. This is consistent with previous reports of a lack of mutations in p18 and p19 in primary human tumors and tumor-derived cell lines, which harbored p16 and p15 mutations [Zariwala and Xiong, 1996]. Defects in INK4 genes would remove cell cycle check-point control, particularly in G1/S phase transition, promoting uncontrolled proliferation. This cancerous phenotype can be at least partially reversed by transfection of human p16 expression constructs into CMT28 cells altering cell phenotype to a less transformed state [DeInnocentes et al., 2009]. The importance of p16/INK4A tumor suppressor defects in promoting CMT28 cell malignancy has been established and appeared coincident with defects in p14ARF and p15. This data suggests that while defects in expression of p16 mRNA in CMT cells are common they may not be sufficient to account for canine mammary neoplasia. Defects in p14ARF and/or p15 in other CMT cell lines suggested further investigation of this locus was warranted as frequency of defects in p15 in human tumors is also lower than p16 [Stone et al., 1995].

We were able to amplify and sequence the entire p16 coding sequence from CMT28 and NCF cells revealing a deletion mutation in p16 exon 1α in CMT28 cells providing a transforming mechanism in this canine mammary tumor model. The mutation in CMT28 p16 would cause failure in expression as the deletion was 17 bp causing a frameshift extending into exon 2. We also determined the partial

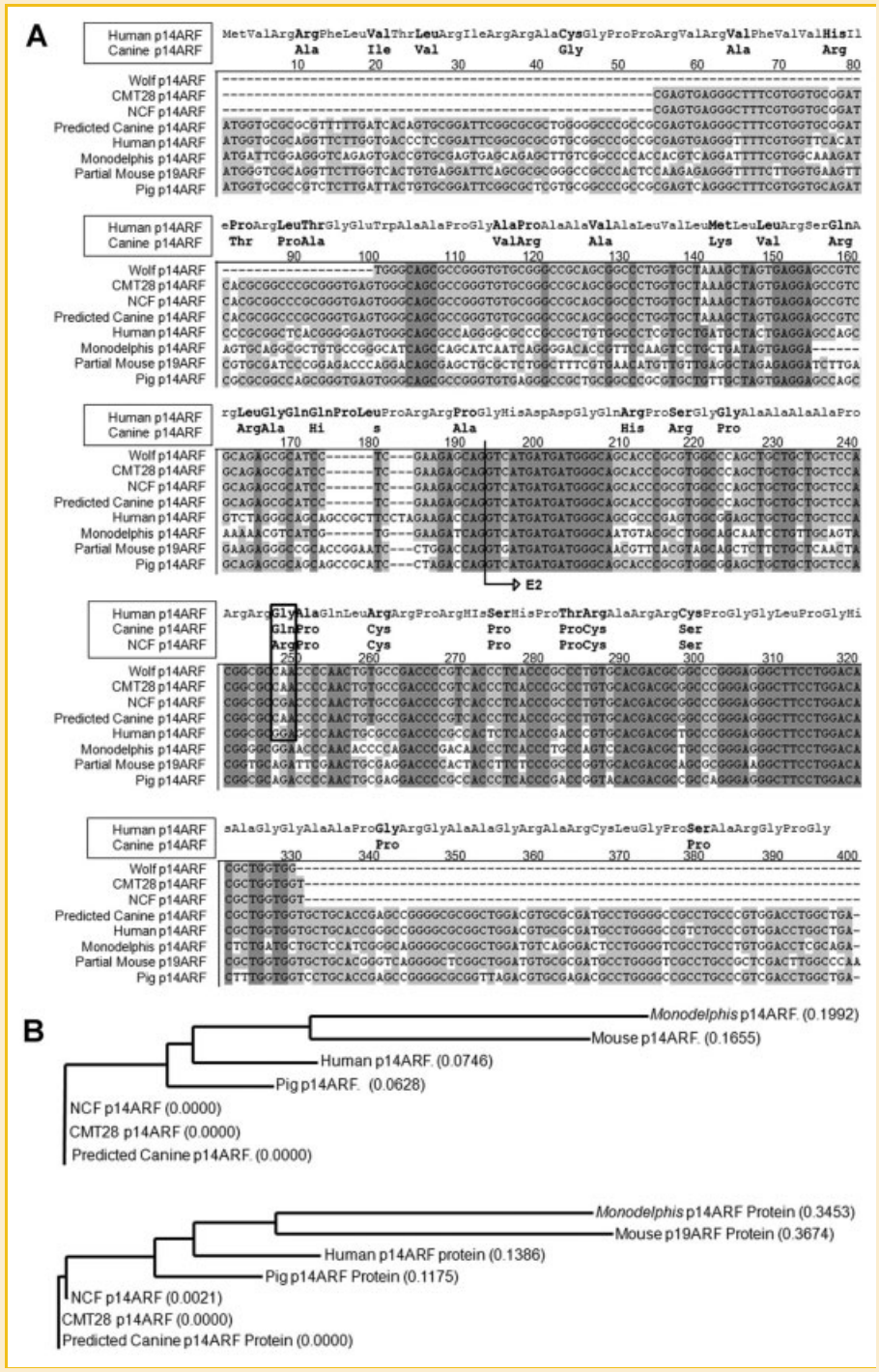

Fig. 4. Alignment of canid p14ARF mRNA sequences from Grey Wolf compared to other mammals. A: Canine and mammalian p14ARF mRNA sequence alignments. Amplicon sequences representing p14 mRNAs from NCF (#JQ801342) and CMT28 (#JQ801341) cells (267 bp), Grey Wolf (*Canis lupus*, #JQ801343) PBMCs (221 bp, nucleotides 56–331 of canine p14ARF ORF encoding amino acids 19–89 of human p14ARF), were cloned, sequenced, aligned and compared to other mammalian p14ARF open reading frames (ORF) including pig (NM213735), *Monodelphis*/Opossum (NM001032973), mouse (NM009877), human (NM058195), and predicted mRNA sequences extrapolated from a partial canine genomic fragment (*C. lupus familiaris* p14ARF gene FM883643). The alignments reveal identical (dark background) and conserved (lighter background) regions and differences between canine and human p14ARF protein sequences are noted (bold). One nucleotide difference between NCF and all other canine sequences resulted in a single allelic difference in amino acid sequence (box). B: Dendrograms of mammalian p14ARF mRNA and protein sequences. The neighbor-joining algorithm was used to calculate a rooted relationship dendrogram for mammalian sequences encoding p14ARF. Published canine, human, rat, mouse, *Monodelphis*, pig, and all of the canine nucleotide and amino acid sequences (CMT28 and NCF cell lines, Grey Wolf PBMCs) were compared. Top: dendrogram of p14ARF mRNA sequences from human, pig, *Monodelphis*, and canids. Bottom: dendrogram of p14ARF protein sequences from human, pig, *Monodelphis*, and canids. Values in parentheses show the length of each branch as described above.

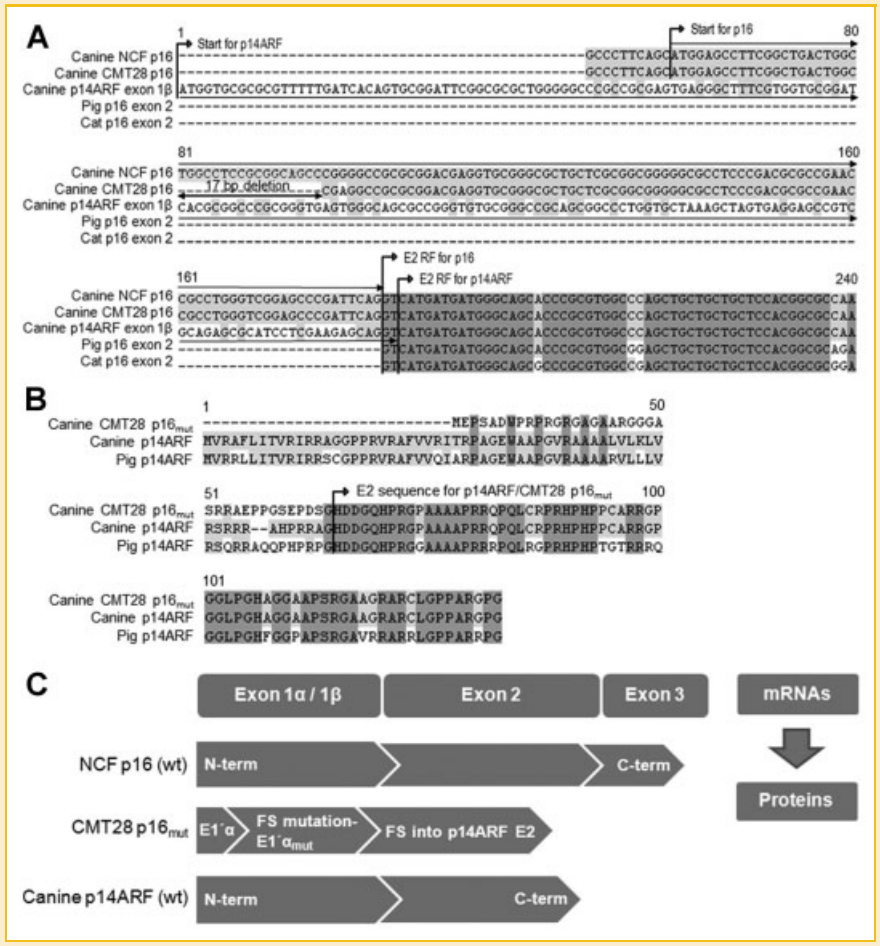

Fig. 5. Mutation of the CMT28 p16 sequence alters the reading frame of exon 2 to p14ARF. A: NCF and CMT28 p16 sequences were compared with p14ARF. Horizontal arrows indicate p16 exon 1α and p14ARF exon 1β reading frames starting from initiation codons (bent arrows labeled ATG). Exon 2 reading frames (bent arrows labeled E2) for NCF p16 or p14ARF are indicated and double-ended arrow indicates CMT28 exon 1α deletion mutation. Alignments of p16, p14ARF and p16 exon 2 are shown. B: Predicted canine (#FM883643) and pig (#AJ510264.1) p14ARF were translated and aligned with CMT28 $p16_{mut}$ and exon 2 boundary noted (bent arrow E2). C: Schematic comparing exon structure of CMT28 $p16_{mut}$ with wild type (wt) canine NCF p16 and p14ARF proteins (FS-frameshift; E1′α-partial exon 1α; N/C term-nitrosal/carboxyl protein termini). Shading of alignments is as for Figure 2.

sequence for the p14ARF open reading frame predicting the canine p14ARF mRNA and protein sequences from NCF, CMT28 and primary *Canus lupus* lymphocytes (Grey Wolf). All canid p14ARF sequences were identical to published canine p14ARF sequences except for a single putative amino acid allelic variant in NCF. When canine p16 and p14ARF nucleotide and protein sequences were compared to other mammals, canine p14ARF sequences were more distant from human p16 sequences. The relationship appeared closer for p16 due to a 3 amino acid deletion/insertion in p14ARF exon 1β in canids and Opossum. Despite these small differences, sequence similarity between canids and humans in the p16/INK4A/p14ARF locus was considerable.

We determined that CMT28 $p16_{mut}$ has an altered reading frame that shifted to that of p14ARF in exon 2 predicting that $p16_{mut}$ would translate into a hybrid protein composed of a short p16 region, a new unique out-of-frame region and a large p14ARF homologous region. The resulting truncated p16/p14 fusion sequence would likely be unstable (index >40) compared to wildtype p16 protein [Gasteiger et al., 2005]. Although this is a theoretical estimate of stability, it has provided a close approximation of stability in vivo [Guruprasad et al., 1990] and likely predicts rapid degradation. This is consistent with reports that CMT28 does not express any detectable p16 protein (Agarwal et al., unpublished data). Two important conclusions can be deduced from comparative protein structure and functional analyses. A loss of function mutation in CMT28 $p16_{mut}$ is likely to disrupt functional integrity including native folding, which is essential for interaction with other proteins. Analysis of p16 and p14ARF suggested that the remarkable co-evolution of these 2 overlapping transcripts has evolved 2 different proteins, largely derived from common nucleotide sequence, that both uniquely contribute to cell proliferation control.

In conclusion, sequencing of open reading frames from the wildtype and mutant canid INK4 locus revealed important aspects of its expression and genetic defects in canine mammary cancer. Mutation altered the reading frame predicting an aberrant fusion protein of p16 and p14ARF predicted to be truncated, unstable, and

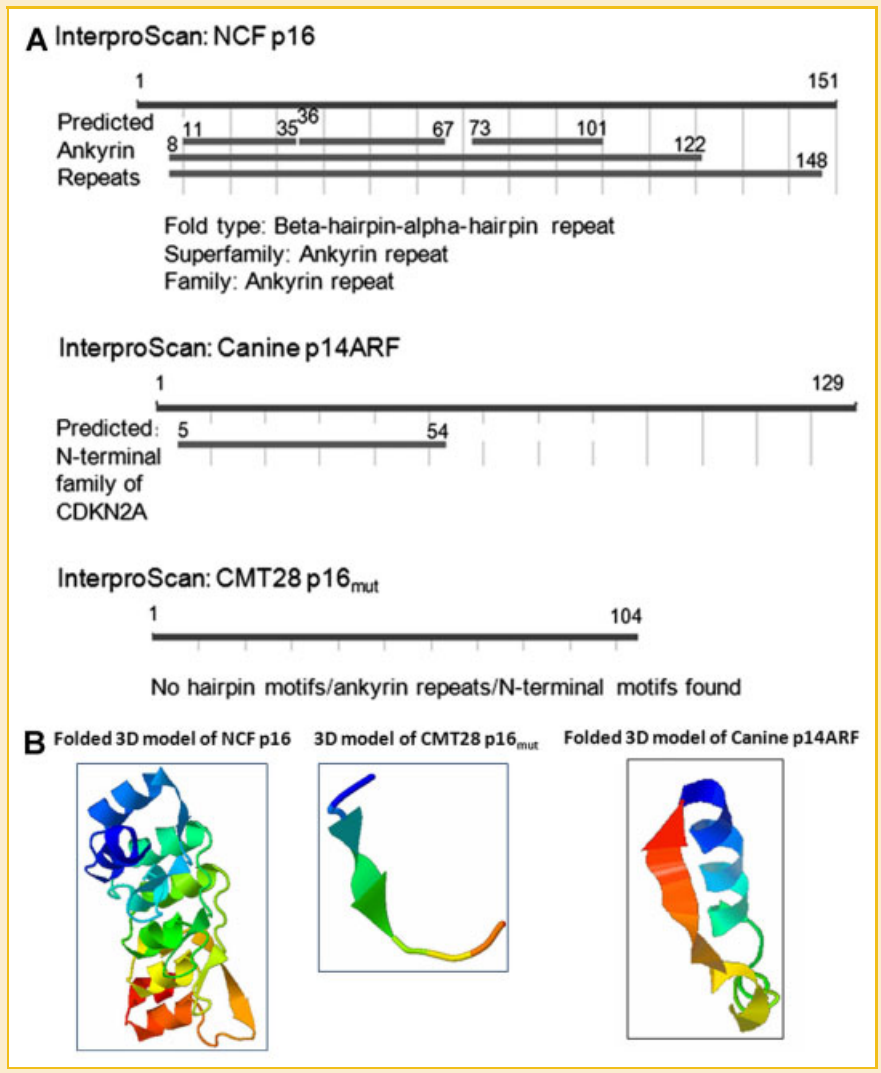

Fig. 6. Comparative analysis of INK4 protein motifs and folding structures. A: NCF p16, CMT28 $p16_{mut}$, and canine p14ARF protein sequences were analyzed by fold/motif recognition tools. Predicted ankyrin repeats and N-terminal motifs are indicated (lines/numbers indicate respective amino acid positions). B: Three dimensional models for NCF p16, CMT28 $p16_{mut}$, and canine p14ARF proteins generated by protein motif recognition tools predicted each protein's folded structure and three dimensional model (Phyre V0.2, 3D-PSSM protein fold recognition servers and Swiss-Model InterProScan tools).

devoid of functional motifs. The loss of function mutation in exon 1α of CMT28 p16 confirmed the critical importance of the INK4A locus in canine mammary cancer. Moreover, the mapping of p16 defects and aberrant expression profiles in the canine breast cancer model should shed light on the mechanisms regulating neoplasia and this important tumor suppressor gene perhaps providing therapeutic insights for human breast cancer.

ACKNOWLEDGMENTS

The authors gratefully acknowledge Dr. Michael Schwitalla and Wild Animal Safari Park, Pine Mountain Georgia, USA for donations of Grey Wolf blood and Dr. Terry Ahern for collaborations developing BTB cells. The authors gratefully acknowledge support from the Animal Health and Disease Research Fund.

REFERENCES

Agarwal P, Lutful Kabir FM, DeInnocentes P, Bird RC. 2012. Tumor suppressor gene p16/INK4A/CDKN2A and its role in cell cycle exit, differentiation, and determination of cell fate. In: Cheng Y, editor Tumor suppressor genes. Rijeka, Croatia: InTech Open Access Pub. pp 1–34.

Ahern TE, Bird RC, Bird AE, Wolfe LG. 1996. Expression of the oncogene c-erbB-2 in canine mammary cancers and tumor-derived cell lines. Am J Vet Res 57:693–696.

Baylin SB, Herman JG, Graff JR, Vertino PM, Issa JP. 1998. Alterations in DNA methylation: A fundamental aspect of neoplasia. Adv Cancer Res 72:141–196.

Bird RC, Deinnocentes P, Church Bird AE, van Ginkel FW, Lindquist J, Smith BF. 2011. An autologous dendritic cell canine mammary tumor hybrid-cell fusion vaccine. Cancer Immunol Immunother 60:87–97.

Bird RC, Deinnocentes P, Lenz S, Thacker EE, Curiel DT, Smith BF. 2008. An allogeneic hybrid-cell fusion vaccine against canine mammary cancer. Vet Immunol Immunopathol 123:289–304.

Boehme KA, Blattner C. 2009. Regulation of p53—Insights into a complex process. Crit Rev Biochem Mol Biol 44:367–392.

Campbell I, Magliocco A, Moyana T, Zheng C, Xiang J. 2000. Adenovirus-mediated p16INK4 gene transfer significantly suppresses human breast cancer growth. Cancer Gene Ther 7:1270–1278.

DeInnocentes P, Agarwal P, Bird RC. 2009. Phenotype-rescue of cyclin-dependent kinase inhibitor p16/INK4A defects in a spontaneous canine cell model of breast cancer. J Cell Biochem 106:491–505.

DeInnocentes P, Li LX, Sanchez RL, Bird RC. 2006. Expression and sequence of canine SIRT2 and p53 genes in canine mammary tumour cells—Effects on downstream targets Wip1 and p21/Cip1. Vet Comp Oncol 4:161–177.

Fosmire SP, Thomas R, Jubala CM, Wojcieszyn JW, Valli VE, Getzy DM, Smith TL, Gardner LA, Ritt MG, Bell JS, Freeman KP, Greenfield BE, Lana SE, Kisseberth WC, Helfand SC, Cutter GR, Breen M, Modiano JF. 2007. Inactivation of the p16 cyclin-dependent kinase inhibitor in high-grade canine non-Hodgkin's T-cell lymphoma. Vet Pathol 44:467–478.

Gasteiger E, Hoogland C, Gattiker A, Duvaud S, Wilkins MR, Appel RD, Bairoch A. 2005. Protein identification and analysis tools on the ExPASy server. In: Walker JM, editor The proteomics protocols handbook. New Jersey: Humana Press. pp 571–607.

Guruprasad K, Reddy BV, Pandit MW. 1990. Correlation between stability of a protein and its dipeptide composition: A novel approach for predicting in vivo stability of a protein from its primary sequence. Protein Eng 4:155–161.

Jin X, Nguyen D, Zhang WW, Kyritsis AP, Roth JA. 1995. Cell cycle arrest and inhibition of tumor cell proliferation by the p16INK4 gene mediated by an adenovirus vector. Cancer Res 55:3250–3253.

Kelley LA, MacCallum RM, Sternberg MJ. 2000. Enhanced genome annotation using structural profiles in the program 3D-PSSM. J Mol Biol 299:499–520.

Kelley LA, Sternberg MJ. 2009. Protein structure prediction on the Web: A case study using the Phyre server. Nat Protoc 4:363–371.

Kim WY, Sharpless NE. 2006. The regulation of INK4/ARF in cancer and aging. Cell 127:265–275.

Kinzler KW, Vogelstein B. 1997. Cancer-susceptibility genes. Gatekeepers and caretakers. Nature 386:761 763.

Koenig A, Bianco SR, Fosmire S, Wojcieszyn J, Modiano JF. 2002. Expression and significance of p53, rb, p21/waf-1, p16/ink-4a, and PTEN tumor suppressors in canine melanoma. Vet Pathol 39:458–472.

Korbie DJ, Mattick JS. 2008. Touchdown PCR for increased specificity and sensitivity in PCR amplification. Nat Protoc 3:1452–1456.

Levine RA, Fleischli MA. 2000. Inactivation of p53 and retinoblastoma family pathways in canine osteosarcoma cell lines. Vet Pathol 37:54–61.

Lindblad-Toh K, Wade CM, Mikkelsen TS, Karlsson EK, Jaffe DB, Kamal M, Clamp M, Chang JL, Kulbokas EJ III, Zody MC, Mauceli E, Xie X, Breen M, Wayne RK, Ostrander EA, Ponting CP, Galibert F, Smith DR, DeJong PJ, Kirkness E, Alvarez P, Biagi T, Brockman W, Butler J, Chin CW, Cook A, Cuff J, Daly MJ, DeCaprio D, Gnerre S, Grabherr M, Kellis M, Kleber M, Bardeleben C, Goodstadt L, Heger A, Hitte C, Kim L, Koepfli KP, Parker HG, Pollinger JP, Searle SM, Sutter NB, Thomas R, Webber C, Baldwin J, Abebe A, Abouelleil A, Aftuck L, Ait-Zahra M, Aldredge T, Allen N, An P, Anderson S, Antoine C, Arachchi H, Aslam A, Ayotte L, Bachantsang P, Barry A, Bayul T, Benamara M, Berlin A, Bessette D, Blitshteyn B, Bloom T, Blye J, Boguslavskiy L, Bonnet C, Boukhgalter B, Brown A, Cahill P, Calixte N, Camarata J, Cheshatsang Y, Chu J, Citroen M, Collymore A, Cooke P, Dawoe T, Daza R, Decktor K, DeGray S, Dhargay N, Dooley K, Dooley K, Dorje P, Dorjee K, Dorris L, Duffey N, Dupes A, Egbiremolen O, Elong R, Falk J, Farina A, Faro S, Ferguson D, Ferreira P, Fisher S, FitzGerald M., et al. 2005. Genome sequence, comparative analysis and haplotype structure of the domestic dog. Nature 438:803–819.

McKeller RN, Fowler JL, Cunningham JJ, Warner N, Smeyne RJ, Zindy F, Skapek SX. 2002. The Arf tumor suppressor gene promotes hyaloid vascular regression during mouse eye development. Proc Natl Acad Sci USA 99:3848–3853.

Migone F, Deinnocentes P, Smith BF, Bird RC. 2006. Alterations in CDK1 expression and nuclear/nucleolar localization following induction in a spontaneous canine mammary cancer model. J Cell Biochem 98:504–518.

Morgan DO. 1997. Cyclin-dependent kinases: Engines, clocks, and microprocessors. Annu Rev Cell Dev Biol 13:261–291.

Oesterreich S, Fuqua SA. 1999. Tumor suppressor genes in breast cancer. Endocr Relat Cancer 6:405–419.

Pines J, Hunter T. 1991. Cyclin-dependent kinases: A new cell cycle motif? Trends Cell Biol 1:117–121.

Ruas M, Peters G. 1998. The p16INK4a/CDKN2A tumor suppressor and its relatives. Biochim Biophys Acta 1378:F115–177.

Russo AA, Tong L, Lee JO, Jeffrey PD, Pavletich NP. 1998. Structural basis for inhibition of the cyclin-dependent kinase Cdk6 by the tumour suppressor p16INK4a. Nature 395:237–243.

Rutteman GR, Withrow SJ, MacEwen EG. 2001. Tumors of the mammary gland. In: Withrow SJ, MacEwen EG, editors. Small animal clinical oncology. Philadelphia: WB Saunders. pp 455–477.

Sharpless NE. 2005. INK4a/ARF: A multifunctional tumor suppressor locus. Mutat Res 576:22–38.

Smith BF, Bird RC. 2010. Hematologic neoplasia—Gene therapy. In: Weiss DJ, Wardrop KJ, editors. Schalm's veterinary hematology. Iowa: Wiley-Blackwell. pp 550–557.

Spillare EA, Okamoto A, Hagiwara K, Demetrick DJ, Serrano M, Beach D, Harris CC. 1996. Suppression of growth in vitro and tumorigenicity in vivo of human carcinoma cell lines by transfected p16INK4. Mol Carcinog 16: 53–60.

Stone S, Dayananth P, Jiang P, Weaver-Feldhaus JM, Tavtigian SV, Cannon-Albright L, Kamb A. 1995. Genomic structure, expression and mutational analysis of the P15 (MTS2) gene. Oncogene 11:987–991.

Tripathy D, Benz CC. 1992. Activated oncogenes and putative tumor suppressor genes involved in human breast cancers. Cancer Treat Res 63:15–60.

Vidal A, Koff A. 2000. Cell-cycle inhibitors: Three families united by a common cause. Gene 247:1–15.

Wass MN, Kelley LA, Sternberg MJ. 2010. 3DLigandSite: Predicting ligand-binding sites using similar structures. Nucleic Acids Res 38:W469–473.

Weber JD, Jeffers JR, Rehg JE, Randle DH, Lozano G, Roussel MF, Sherr CJ, Zambetti GP. 2000. p53-independent functions of the p19(ARF) tumor suppressor. Genes Dev 14:2358–2365.

Weinberg RA. 1995. The retinoblastoma protein and cell cycle control. Cell 81:323–330.

Withrow SJ, MacEwen EG. 1996. Small animal clinical oncology. Philadelphia: WB Saunders. pp 589.

Wolfe LG, Smith BB, Toivio-Kinnucan MA, Sartin EA, Kwapien RP, Henderson RA, Barnes S. 1986. Biologic properties of cell lines derived from canine mammary carcinomas. J Natl Cancer Inst 77:783–792.

You J, Bird RC. 1995. Selective induction of cell cycle regulatory genes cdk1 (p34cdc2), cyclins A/B, and the tumor suppressor gene Rb in transformed cells by okadaic acid. J Cell Physiol 164:424–433.

Zariwala M, Xiong Y. 1996. Lack of mutation in the cyclin-dependent kinase inhibitor, p19INK4d, in tumor-derived cell lines and primary tumors. Oncogene 13:2033–2038.

Zdobnov EM, Apweiler R. 2001. InterProScan—An integration platform for the signature-recognition methods in InterPro. Bioinformatics 17:847–848.